

Nature of the band gap of Tl_2O_3

Aoife B. Kehoe, David O. Scanlon,^{*} and Graeme W. Watson[†]*School of Chemistry and CRANN, Trinity College Dublin, Dublin 2, Ireland*

(Received 11 February 2011; revised manuscript received 13 April 2011; published 9 June 2011)

The ground state electronic structure of thallic oxide has been a source of controversy in the literature, with Tl_2O_3 reported to be either a degenerate *n*-type semiconductor or an intrinsic semimetal with no band gap. Using a screened hybrid density functional theory (DFT) approach, we show that Tl_2O_3 is a semiconductor with a predicted band gap of 0.33 eV. We rationalize the large optical band gaps reported in experimental studies and demonstrate that previous “standard” DFT approaches wrongly predict Tl_2O_3 to be a semimetal. Doubly ionized oxygen vacancies are shown to be the origin of the high carrier concentrations seen experimentally.

DOI: [10.1103/PhysRevB.83.233202](https://doi.org/10.1103/PhysRevB.83.233202)

PACS number(s): 71.20.Nr, 71.55.-i

Thallic oxide (Tl_2O_3) is a brown/black material that adopts the body-centered cubic bixbyite (FeMnO_3) structure below 600 °C.¹ It possesses a very low resistivity ($\sim 10^{-4} \Omega \text{ cm}^{-1}$), and has previously been utilized as an electrode in high-efficiency solar cells.² Tl_2O_3 has also been studied as a candidate for optical communication applications, as its high carrier concentration means that it possesses a strong reflectance in the 1300–1500 nm region of the near-infrared.³

Despite its extremely high *n*-type conductivity,⁴ the electronic structure of Tl_2O_3 is still a cause for much debate.^{3,5,6} It has been postulated for decades that Tl_2O_3 is a metallic conductor,^{5–7} but conversely the carrier concentration is found to vary strongly with oxygen partial pressure,^{7–10} which is indicative of a defect induced, semiconducting nature. The arguments that Tl_2O_3 is a semiconductor have been supported by the fact that many studies have reported it to possess optical band gaps varying from 1.40 to 2.75 eV.^{3,5,8}

Geserich reported the direct band gap of Tl_2O_3 to be 2.20 eV, with an indirect band gap of 1.40 eV.⁵ Van Leeuwen *et al.* found that the indirect optical band gap of electrodeposited Tl_2O_3 ranged from 1.65 to 1.70 eV with applied overpotentials of 300 and 44 mV, respectively.³ The corresponding direct transitions were determined to be 2.57 and 2.75 eV. Based on the band structure model suggested in their study, Van Leeuwen *et al.* stated that the fundamental band gap [i.e., from the valence band maximum (VBM) to the conduction band minimum (CBM)], can be calculated as the difference between the Fermi energy and the indirect band gap.³ The authors reported that E_F was 1.15 eV (1.04 eV) above the CBM, for an overpotential of 300 mV (44 mV), and suggested a fundamental band gap of 0.50 eV (0.66 eV). It should be noted that these fundamental band gaps are very dependent on the model used by Van Leeuwen *et al.*, and is by no means actually measured or definitive. Shukla and Wirtz⁸ reported the optical band gap of Tl_2O_3 to be 1.4 eV, and attributed the presence of donor states to native defects, since the carrier concentration was greater than the impurity concentration by 2 orders of magnitude.

Recently, the electronic structure of Tl_2O_3 was studied by Glans *et al.* using valence and core-level x-ray photoemission, x-ray absorption, and x-ray emission spectroscopies, together with DFT calculations.⁶ The photoemission spectrum of Tl_2O_3 showed a well-defined metallic Fermi edge, in accord with the bulk transport properties. However, the edge of the main

valence band (VB) was found to be ~ 1.1 eV below the Fermi energy.⁶ DFT calculations using the generalized gradient approximation (GGA) of Perdew, Burke, and Ernzerhof [PBE (Ref. 11)] predicted Tl_2O_3 to be intrinsically metallic, as the density of states did not go to zero at the Fermi energy, which was found to be just above the VB edge.⁶ Thus, although both experiment and theory predicted metallic behavior, the positions of the Fermi energy relative to the VB were at variance. This discrepancy was attributed to excess electrons introduced into the material by some type of *n*-type defects, probably self-doping due to oxygen vacancy formation.⁶

In this Brief Report, we investigate the electronic structure of Tl_2O_3 using GGA-PBE and the screened hybrid density functional as proposed by Heyd, Scuzeria, and Ernzerhof [HSE06 (Ref. 12)]. We demonstrate the previous prediction of Tl_2O_3 being intrinsically metallic is a result of the band gap errors inherent in “standard” DFT functionals such as GGA/LDA. HSE06 results indicate that the fundamental band gap of Tl_2O_3 is semiconducting in nature, and predict it to be 0.33 eV. Tl_2O_3 is found to have disallowed transitions from VBM to CBM, similar to isoelectronic bixbyite In_2O_3 , with the absorption allowed from bands ~ 1.17 eV below the VBM. We rationalize the large optical band gaps reported in the literature, and from our calculations propose a new model to understand optical band gaps in Tl_2O_3 . Finally, we show the source of the high carrier concentrations in Tl_2O_3 is doubly ionized oxygen vacancies.

All our DFT calculations were performed using the VASP code,¹³ with interactions between the cores (Tl:[Xe] and O:[He]) and the valence electrons were described using the PAW method.¹⁴ The calculations were performed using both PBE (Ref. 11) and the hybrid functional as proposed by HSE06 (Ref. 12). In the HSE06 approach, a value of exact nonlocal exchange, α , of 25%, and screening parameter of $\omega = 0.11 \text{ bohr}^{-1}$ are added to the PBE formalism. The HSE approach has been proven to result in structural and band gap data in better agreement with experiment than standard DFT functionals.^{15–23} A planewave cutoff of 400 eV and a *k*-point sampling of Γ centered $3 \times 3 \times 3$ for the 40 atom primitive cell of Tl_2O_3 were used, with the structure deemed to be converged when the forces on all the atoms were less than $0.01 \text{ eV } \text{Å}^{-1}$. The optical transition matrix elements and the optical absorption spectrum were calculated within the transversal approximation.²⁴ Within this methodology,

the adsorption spectra is summed over all direct VB to CB transitions and therefore ignores indirect and intraband adsorptions.²⁵ Defects were calculated in the 80-atom bixbyite cell, and all calculations were spin polarized. The formation enthalpy of a defect with charge state q is given by

$$\Delta H_f(D,q) = (E^{D,q} - E^H) + \sum_i n_i (E_i + \mu_i) + q(E_{\text{Fermi}} + \epsilon_{\text{VBM}}^H) + E_{\text{align}}[q], \quad (1)$$

where E^H is the total energy of the stoichiometric host supercell and $E^{D,q}$ is the total energy of the defective cell. Elemental reference energies, E_i , were obtained from calculations on the constituent elements in their standard states, i.e., $\text{Ti}_{(s)}$ and $\text{O}_{2(g)}$, and n is the number of atoms formally added to, or taken away, from an external reservoir. E_{Fermi} ranges from the VBM ($E_{\text{Fermi}} = 0 \text{ eV}$) to the CBM. ϵ_{VBM}^H is the VBM eigenvalue of the host bulk. $E_{\text{align}}[q]$ is a correction that (i) accounts for the proper alignment of the VBM between the bulk and the defective supercells and (ii) corrections for the finite-size-cell effects in the calculations of charged impurities, as outlined by Freysoldt *et al.*²⁶ A correction for band filling by shallow donors was also included.²⁷ The chemical potential limit of the *O-poor/Ti-rich* conditions were checked, with Ti_2O formation found to be a bounding condition. The thermodynamic transition (ionization) levels (TLs) of a given defect, $\epsilon_D(q/q')$, are equal to the Fermi level for which charge states q and q' have equal energy:

$$\epsilon_D(q/q') = \frac{\Delta H^f(D,q) - \Delta H^f(D,q')}{q' - q} \quad (2)$$

The PBE and HSE06 calculated lattice constants for Ti_2O_3 are 10.78 and 10.56 Å, respectively. PBE overestimates the experimental lattice constants by $\sim 2.3\%$, whereas HSE06 only overestimates by only $\sim 0.02\%$. The PBE and HSE06 calculated total and partial electronic density of states (PEDOS) for Ti_2O_3 are shown in Fig. 1. The general features are the same for both methods; the main Ti 5d peak is split off from the bottom of the valence band, the VB is dominated by O 2p states, with small contributions from the Ti 6p, 5d, and 6s, and the bottom of the conduction band is predominantly of

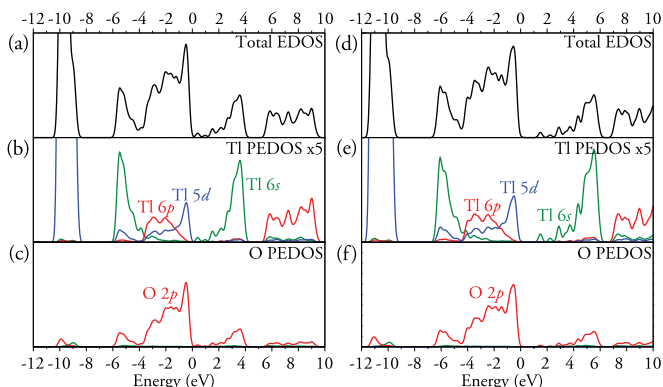


FIG. 1. (Color online) The total and partial density of states for Ti_2O_3 as calculated with (a) PBE and (b) HSE06. The scale on which the Ti 6s, 6p, and 5d states are presented is increased by a factor of 5. The highest occupied state is set to 0 eV.

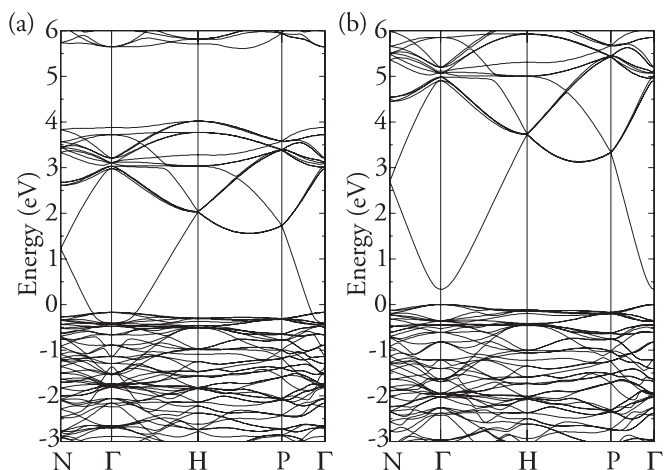


FIG. 2. The band structure of Ti_2O_3 as calculated with (a) PBE and (b) HSE06. The highest occupied state is set to 0 eV.

Ti 6s character with some minor O 2p contributions. The main differences between the two methods are that in the HSE06 results: (i) the main Ti 5d peak is pushed downward in energy relative to the VBM, (ii) the VB width is slightly increased, and (iii) a band gap has opened up between the O 2p states and the Ti 6s states. The PBE PEDOS does not display any band gap, consistent with Ti_2O_3 being metallic.

To examine the band gap issue further, the PBE and HSE06 calculated band structure using the special k -points taken from of Bradley and Cracknell²⁸ are shown in Figs. 2(a) and 2(b). It is clear that, for the PBE band structure, the conduction band overlaps with the valence band, which is typical of a semimetallic material. The HSE06 band structure, however, is quite different. The VBM and CBM both appear at the Γ point, and are separated by 0.33 eV. HSE06 therefore predicts Ti_2O_3 to be a semiconductor, with a definite band gap. The HSE06 band gap is slightly smaller than the fundamental band gap estimated by Van Leeuwen *et al.*, and is significantly smaller than the literature optical band gaps of 1.4–2.75 eV.^{3,5,8} HSE06 has been shown to underestimate the band gaps of other wide band gap n -type oxides, e.g., ZnO and SnO_2 ;^{29,30} however, it has been shown to be quite accurate for isoelectronic In_2O_3 .³¹ It is therefore likely that our HSE06 calculated band gap suggested for Ti_2O_3 is slightly underestimated. An experimental reinvestigation of the fundamental band gap of Ti_2O_3 is therefore warranted to assess the accuracy of our prediction.

To investigate the discrepancy between our small calculated fundamental band gap and the large optical band gaps from experiment, we have computed the optical absorption spectra for Ti_2O_3 with HSE06, with the results presented in Fig. 3(a). The onset of optical absorption begins at $\sim 1.50 \text{ eV}$ and increases steadily. The reason for the large difference between the optical band gap and the fundamental band gap can be explained by analyzing the allowed transitions from the valence band to the conduction band. The onset of optical absorption does not begin until $\sim 1.17 \text{ eV}$ below the VBM at Γ [Fig. 3(b)] as transitions above this point are symmetry forbidden. This type of behavior has recently been reported for isoelectronic In_2O_3 , which was shown to possess a fundamental band gap of $\sim 2.90 \text{ eV}$, and an optical band gap of 3.75 eV.³² Walsh *et al.* demonstrated that transitions from the VBM to the CBM

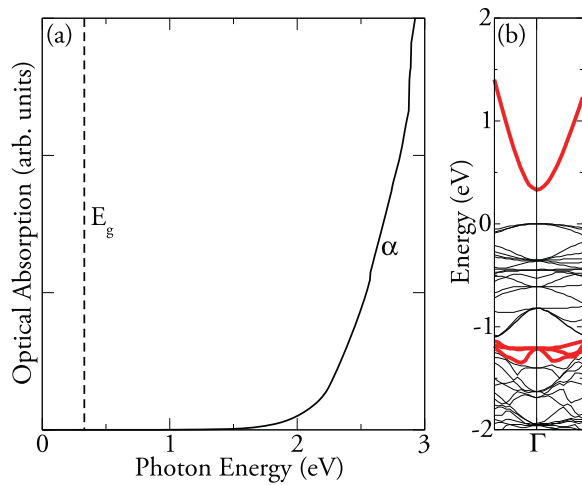


FIG. 3. (Color online) (a) Calculated absorption spectrum of bulk Tl_2O_3 . Note the onset of optical absorption is ~ 1.2 eV above the fundamental band gap. (b) Band structure of Tl_2O_3 (along the $\text{H}-\Gamma-\text{N}$ lines). The highest energy valence bands resulting in strong optical absorption to the conduction band are bold gray (red).

of In_2O_3 are symmetry disallowed,³² with optical absorption only occurring from bands 0.80 eV below the VBM.

Although the HSE06 calculations indicate that the optical band gap is ~ 1.50 eV, this cannot explain the optical band gaps reported in the literature in the range 1.4–2.75 eV.^{3,5,8} This can be rationalized if we recall that the Fermi level, E_F , of the samples reported by Egdell and co-workers was found to be ~ 1.1 eV above the VB edge.⁶ Taking into account a fundamental band gap of 0.33 eV from our HSE calculations, and ignoring any band gap renormalization effects,³³ this would suggest a Burstein-Moss shift of about 0.77 eV. In fact, a Burstein-Moss shift of 0.74 eV has been reported for Tl_2O_3 single crystals at low oxygen partial pressures.¹⁰ Based on our revised model for the semiconducting nature of Tl_2O_3 , this would suggest that the optical band gap could be of the order of ~ 2.3 eV, as indicated in Fig. 4. The height of the E_F above the VBM has even been predicted to be as high as 1.65 eV,³ indicating that the optical band gap could extend up to ~ 2.8 eV, which would explain the higher optical band gaps reported previously.

A Burstein-Moss shift of such a large magnitude would generally be consistent with some sort of extrinsic doping to raise the carrier concentrations. The samples investigated by Egdell and co-workers were, however, not exposed to any extrinsic doping.⁶ Previous studies on Tl_2O_3 have also noted that the carrier concentrations display strong oxygen partial pressure dependence, indicating that ionized oxygen vacancies, V_O could play a role.¹⁰ It has been found, however, that V_O in other degenerate n -type oxides acts as a deep donor (e.g., SnO_2 , ZnO , and In_2O_3).^{30,31,34–36} We have therefore investigated the formation of oxygen vacancies in Tl_2O_3 using HSE06, and find that the V_O always acts as a shallow donor in Tl_2O_3 , with the only V_O^{+2} charge state being stable in the band gap (Fig. 5). The formation energy for the neutral V_O under O -rich/ Tl -poor conditions is 0.8 eV, and only 0.01 eV under O -poor/ Tl -rich (reducing) conditions. In ZnO , SnO_2 , and In_2O_3 , the formation energy of V_O under reducing

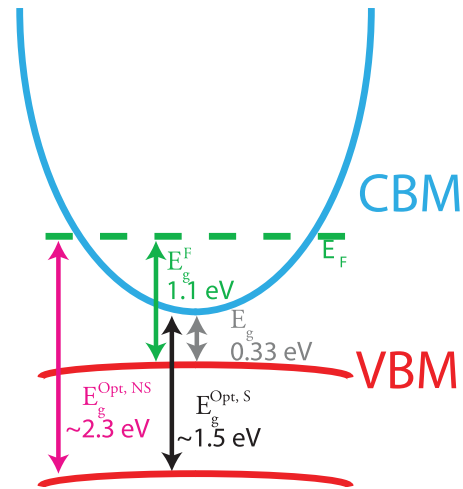


FIG. 4. (Color online) Schematic of the optical absorption of Tl_2O_3 seen experimentally. E_g represents the fundamental band gap as calculated with HSE06, $E_g^{\text{Opt},S}$ represents the HSE06 calculated onset of optical absorption for stoichiometric Tl_2O_3 , E_g^F represents the distance of the E_F from the VBM reported in Ref. 6, and $E_g^{\text{Opt},NS}$ represents the total optical absorption of a nonstoichiometric Tl_2O_3 sample.

conditions is generally ~ 0.8 – 1.1 eV.^{30,34,37} This indicates that Tl_2O_3 samples will be likely to contain a high level of sub stoichiometry on the oxygen sublattice, and thus the origin of the high carrier concentration of Tl_2O_3 is most likely doubly ionized V_O . Our results compare nicely with previous experiments which found Tl_2O_3 samples to always be oxygen deficient.⁷

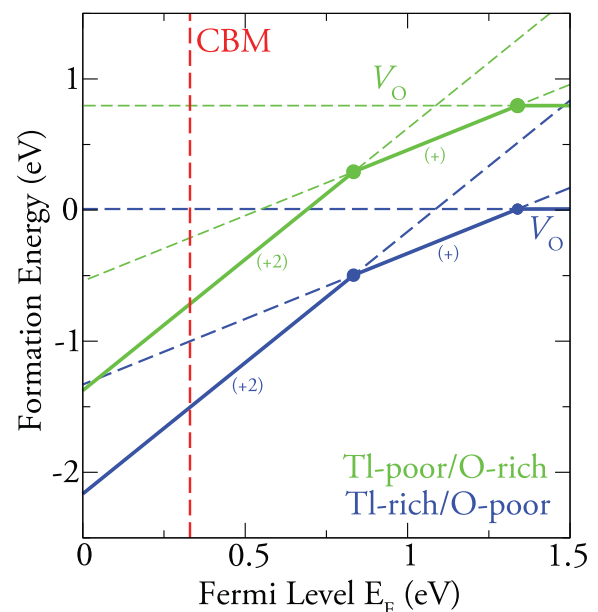


FIG. 5. (Color online) HSE06 calculated formation energies for V_O under Tl -rich/ O -poor conditions [dark gray (blue)] and Tl -poor/ O -rich [light grey (green)] conditions. The solid dots denote the transition levels $\epsilon(q/q')$. The HSE06 calculated CBM is indicated by the vertical (red) dashed line.

We have demonstrated using hybrid DFT that Ti_2O_3 is a semiconductor with a suggested fundamental direct band gap of 0.33 eV at the Γ point, and not a semimetal as standard DFT functionals and some experiments had predicted. Optical transitions from the VBM to the CBM are symmetry disallowed with the onset of optical absorption only allowed from bands ~ 1.17 eV below the VBM to the CBM. The large optical band gaps reported experimentally can be understood as a combination of the disallowed transitions and a large

Burnstein-Moss shift in the conduction band. The origin of the large charge carrier concentration causing the Burnstein-Moss shift is found to be doubly ionized V_{O} .

This work was supported by SFI through the PI programme (PI Grant Nos. 06/IN.1/I92 and 06/IN.1/I92/EC07). Calculations were performed on the IITAC, Lonsdale and Kelvin clusters as maintained by TCHPC, and the Stokes cluster as maintained by ICHEC.

*scanloda@tcd.ie

†watsong@tcd.ie

¹P. Papamantellos, *Z. Kristallogr.* **126**, 143 (1968).

²J. A. Switzer, *J. Electrochem. Soc.* **133**, 722 (1986).

³R. A. Van Leeuwen, C. J. Hung, D. R. Kammler, and J. A. Switzer, *J. Phys. Chem.* **99**, 15247 (1995).

⁴R. J. Phillips, M. J. Shane, and J. A. Switzer, *J. Mater. Res.* **4**, 923 (1989).

⁵H. P. Geserich, *Phys. Status Solidi* **25**, 741 (1968).

⁶P. A. Glans, T. Learmonth, K. E. Smith, J. Guo, A. Walsh, G. W. Watson, F. Terzi, and R. G. Egdell, *Phys. Rev. B* **71**, 235109 (2005).

⁷A. Goto, H. Yasuoka, A. Hayashi, and Y. Ueda, *J. Phys. Soc. Jpn.* **61**, 1178 (1992).

⁸V. N. Shukla and G. P. Wirtz, *J. Am. Ceram. Soc.* **60**, 253 (1977).

⁹V. N. Shukla and G. P. Wirtz, *J. Am. Ceram. Soc.* **60**, 259 (1977).

¹⁰G. P. Wirtz, C. J. Yu, and R. W. Doser, *J. Am. Ceram. Soc.* **64**, 269 (1981).

¹¹J. P. Perdew, K. Burke, and M. Ernzerhof, *Phys. Rev. Lett.* **77**, 3865 (1996).

¹²A. V. Krukau, O. A. Vydrov, A. F. Izmaylov, and G. E. Scuseria, *J. Chem. Phys.* **125**, 224106 (2006).

¹³G. Kresse and J. Furthmüller, *Phys. Rev. B* **54**, 11169 (1996).

¹⁴G. Kresse and D. Joubert, *Phys. Rev. B* **59**, 1758 (1999).

¹⁵J. P. Allen, D. O. Scanlon, and G. W. Watson, *Phys. Rev. B* **81**, 161103(R) (2010).

¹⁶A. Stroppa and G. Kresse, *Phys. Rev. B* **79**, 201201(R) (2009).

¹⁷A. Stroppa and S. Picozzi, *Phys. Chem. Chem. Phys.* **12**, 5405 (2010).

¹⁸I. D. Prodan, G. E. Scuseria, and R. L. Martin, *Phys. Rev. B* **73**, 045104 (2006).

¹⁹B. G. Janesko, T. M. Henderson, and G. E. Scuseria, *Phys. Chem. Chem. Phys.* **11**, 443 (2009).

²⁰J. E. Peralta, J. Heyd, G. E. Scuseria, and R. L. Martin, *Phys. Rev. B* **74**, 073101 (2006).

²¹D. O. Scanlon and G. W. Watson, *J. Phys. Chem. Lett.* **1**, 2582 (2010).

²²D. O. Scanlon and G. W. Watson, *J. Phys. Chem. Lett.* **1**, 3195 (2010).

²³D. O. Scanlon, B. J. Morgan, G. W. Watson, and A. Walsh, *Phys. Rev. Lett.* **103**, 096405 (2009).

²⁴M. Gajdos, K. Hummer, G. Kresse, J. Furthmüller, and F. Bechstedt, *Phys. Rev. B* **73**, 045112 (2006).

²⁵B. Adolph, J. Furthmüller, and F. Bechstedt, *Phys. Rev. B* **63**, 125108 (2001).

²⁶C. Freysoldt, J. Neugebauer, and C. G. Van de Walle, *Phys. Rev. Lett.* **102**, 016402 (2009).

²⁷S. Lany and A. Zunger, *Phys. Rev. B* **78**, 235104 (2008).

²⁸C. J. Bradley and A. P. Cracknell, *The Mathematical Theory of Symmetry in Solids* (Clarendon, Oxford, 1972).

²⁹J. B. Varley, A. Janotti, A. K. Singh, and C. G. Van de Walle, *Phys. Rev. B* **79**, 245206 (2009).

³⁰S. J. Clark, J. Robertson, S. Lany, and A. Zunger, *Phys. Rev. B* **81**, 115311 (2010).

³¹P. Agoston, K. Albe, R. M. Nieminen, and M. J. Puska, *Phys. Rev. Lett.* **103**, 245501 (2009).

³²A. Walsh, J. L. F. Da Silva, S. H. Wei, C. Korber, A. Klein, L. F. J. Piper, A. DeMasi, K. E. Smith, G. Panaccione, P. Torelli *et al.*, *Phys. Rev. Lett.* **100**, 167402 (2008).

³³A. Walsh, J. L. F. Da Silva, and S. H. Wei, *Phys. Rev. B* **78**, 075211 (2008).

³⁴A. K. Singh, A. Janotti, M. Scheffler, and C. G. Van de Walle, *Phys. Rev. Lett.* **101**, 055502 (2008).

³⁵S. Lany and A. Zunger, *Phys. Rev. Lett.* **106**, 069601 (2011).

³⁶P. Agoston, K. Albe, R. M. Nieminen, and M. J. Puska, *Phys. Rev. Lett.* **106**, 069602 (2011).

³⁷S. Limpijumng, P. Reunchan, A. Janotti, and C. G. Van de Walle, *Phys. Rev. B* **80**, 193202 (2009).